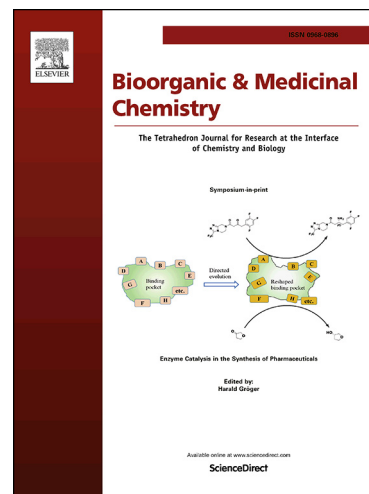


Accepted Manuscript

Discovery of a crystalline sulforaphane analog with good solid-state stability and engagement of the Nrf2 pathway *in vitro* and *in vivo*

Jeffrey Boehm, Roderick Davis, Claudia E. Murar, Tindy Li, Brent McClelland, Shuping Dong, Hongxing Yan, Jeffrey Kerns, Christopher J. Moody, Anthony J. Wilson, Alan P. Graves, Mary Mentzer, Hongwei Qi, John Yonchuk, Jen-Pyng Kou, Joseph Foley, Yolanda Sanchez, Patricia L. Podolin, Brian Bolognese, Catherine Booth-Genthe, Marc Galop, Lawrence Wolfe, Robin Carr, James F. Callahan



PII: S0968-0896(18)31630-4
DOI: <https://doi.org/10.1016/j.bmc.2018.12.026>
Reference: BMC 14675

To appear in: *Bioorganic & Medicinal Chemistry*

Received Date: 18 September 2018
Revised Date: 6 December 2018
Accepted Date: 15 December 2018

Please cite this article as: Boehm, J., Davis, R., Murar, C.E., Li, T., McClelland, B., Dong, S., Yan, H., Kerns, J., Moody, C.J., Wilson, A.J., Graves, A.P., Mentzer, M., Qi, H., Yonchuk, J., Kou, J-P., Foley, J., Sanchez, Y., Podolin, P.L., Bolognese, B., Booth-Genthe, C., Galop, M., Wolfe, L., Carr, R., Callahan, J.F., Discovery of a crystalline sulforaphane analog with good solid-state stability and engagement of the Nrf2 pathway *in vitro* and *in vivo*, *Bioorganic & Medicinal Chemistry* (2018), doi: <https://doi.org/10.1016/j.bmc.2018.12.026>

This is a PDF file of an unedited manuscript that has been accepted for publication. As a service to our customers we are providing this early version of the manuscript. The manuscript will undergo copyediting, typesetting, and review of the resulting proof before it is published in its final form. Please note that during the production process errors may be discovered which could affect the content, and all legal disclaimers that apply to the journal pertain.

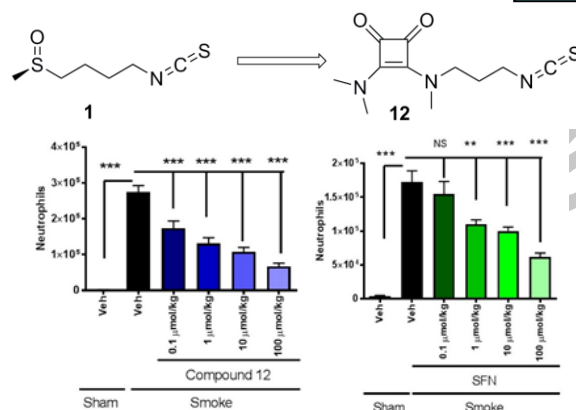
Graphical Abstract

To create your abstract, type over the instructions in the template box below.
Fonts or abstract dimensions should not be changed or altered.

Discovery of a crystalline sulforaphane analog with good solid-state stability and engagement of the Nrf2 pathway *in vitro* and *in vivo*.

Respiratory Stress and Repair Discovery Performance Unit, GSK, Upper Providence, PA 19426, USA

Leave this area blank for abstract info.





ELSEVIER

Bioorganic & Medicinal Chemistry
journal homepage: www.elsevier.com

Discovery of a crystalline sulforaphane analog with good solid-state stability and engagement of the Nrf2 pathway *in vitro* and *in vivo*.

Jeffrey Boehm^{a*}, Roderick Davis^a, Claudia E. Murar^a, Tindy Li^a, Brent McClelland^a, Shuping Dong^a, Hongxing Yan^a, Jeffrey Kerns^a, Christopher J. Moody^c, Anthony J. Wilson^c, Alan P. Graves^b, Mary Mentzer^b, Hongwei Qi^b, John Yonchuk^a, Jen-Pyng Kou^a, Joseph Foley^a, Yolanda Sanchez^a, Patricia L Podolin^a, Brian Bolognese^a, Catherine Booth-Genthe^a, Marc Galop^b, Lawrence Wolfe^b, Robin Carr^a, and James F Callahan^a

^a Respiratory Stress and Repair DPU, GlaxoSmithKline, Upper Providence, PA 19426, USA

^b Platform Technology and Science, GlaxoSmithKline, Upper Merion, PA 19406 and Upper Providence, PA 19426, USA

^c School of Chemistry, University of Nottingham, Nottingham NG7 2RD, U.K.

ARTICLE INFO

Article history:

Received

Received in revised form

Accepted

Available online

Keywords:

Nrf2

KEAP1

Sulforaphane

Isothiocyanate

COPD

* Corresponding author. Tel.: +1-484 923-3596; fax: +1-610-917-4621; e-mail: jeffrey.c.boehm@gsk.com

ABSTRACT.

The antioxidant natural product sulforaphane (SFN) is an oil with poor aqueous and thermal stability. Recent work with SFN has sought to optimize methods of formulation for oral and topical administration. Herein we report the design of new analogs of SFN with the goal of improving stability and drug-like properties. Lead compounds were selected based on potency in a cellular screen and physicochemical properties. Among these, **12** had good aqueous solubility, permeability and long-term solid-state stability at 23 °C. Compound **12** also displayed comparable or better efficacy in cellular assays relative to SFN and had *in vivo* activity in a mouse cigarette smoke challenge model of acute oxidative stress.

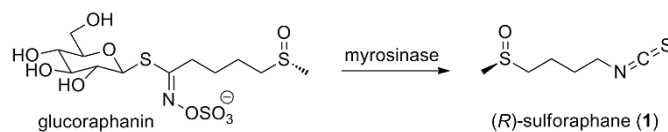
2009 Elsevier Ltd. All rights reserved.

1. Introduction

One of the pathophysiological drivers of Chronic Obstructive Pulmonary Disease (COPD) is the imbalance between biochemical oxidants and antioxidants resulting in oxidative stress that leads to inflammation, tissue damage and emphysema. Levels of expression of antioxidant genes are regulated by Nrf2 (NF-E2-related factor 2) and the associated sequestering protein Kelch-like ECH-associated protein 1 (KEAP1). Activation of the Nrf2 pathway is a potential target for the treatment of COPD.¹ Cytoplasmic Nrf2 binds to the dimeric protein, KEAP1, that targets Nrf2 for Cullin-3 (Cul3) mediated ubiquitination and subsequent proteasome degradation. Under oxidative stress conditions, the KEAP1/Cul3-dependent ubiquitination of Nrf2 is disrupted and Nrf2 accumulates in the cytoplasm of the cell and subsequently translocates to the nucleus leading to the induction of antioxidant and cytoprotective gene expression.^{2,3}

Analogous to the physiological effect of oxidative stress, inactivating KEAP1/Cul3/Nrf2-mediated Nrf2 degradation by reversible-covalent modification of reactive cysteine residues in KEAP1, e.g., Cys151, increases the amount of Nrf2 reaching the nucleus. This is the reported mechanism of Nrf2 activation by many natural and synthetic electrophiles.^{2,4}

Among these different electrophilic Nrf2 activators, natural *R*-sulforaphane (SFN) **1**⁵, is derived by the enzymatic action of myrosinase (β -thioglucosidase) on glucoraphanin found in cruciferous vegetables (**Scheme 1**). Chewing damages the plant tissue which releases compartmentalized myrosinase and glucoraphanin. Myrosinase is also found in the bacterial microflora of the human gastrointestinal tract.⁶ Thus, beneficial antioxidant effects have been attributed to cruciferous vegetables.^{6a,7} Efforts have been made to activate the Nrf2 pathway by administration of both extracts from cruciferous vegetables, as well as synthetic natural or racemic SFN. SFN itself is an oil with poor aqueous stability and therefore the goal of developing synthetic SFN as a drug involves the development of a suitable formulation for oral or topical administration.^{8,9,10,11}



Scheme 1. Sulforaphane is biosynthetically derived from the naturally occurring glucosinolate, glucoraphanin.

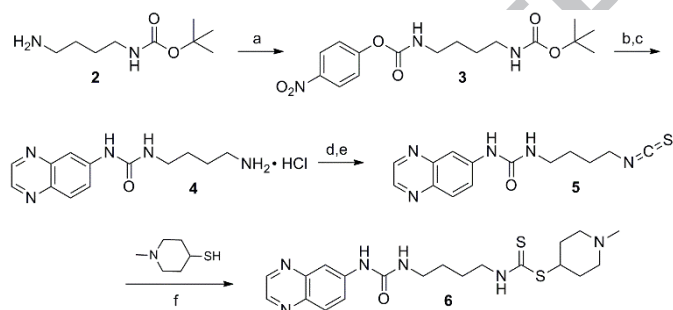
SFN has several additional disadvantages hindering its development as a drug, including relatively low potency in

functional assays which measure the induction of antioxidant proteins and detoxifying enzymes downstream of Nrf2 activation in cellular systems. Furthermore, the fact that natural SFN is a chiral sulfoxide adds complexity to the chemical synthesis of the natural isomer.¹² However, as a lead compound for optimization, SFN does have a low molecular weight (177) and is a polar molecule ($\text{clogP} = 0.15$), leaving many possibilities for modification to improve potency and physicochemical properties. As part of our ongoing efforts to discover novel approaches to the treatment of COPD, we investigated analogs related to SFN with the goal of identifying a molecule with antioxidant-inducing effects comparable or superior to SFN and with enhanced capacity to be readily formulated for oral administration.

2. Results and Discussion

Chemistry

The described isothiocyanates and dithiocarbamates were prepared from primary amine precursors starting with readily available *n*-alkyl diamines with the desired linker. A typical synthesis is depicted in **Scheme 2**. Analogs with a urea such as **5** were synthesized from the *mono*-Boc protected diamines by first preparing the *p*-nitrophenol carbamate **3** with *p*-nitrophenyl chloroformate and then reaction of the activated carbamate with an amine afforded mixed ureas such as **4** after Boc cleavage. There are many methods of isothiocyanate synthesis in the chemical literature and these methods can be optimized for specific structures.¹³ In the present example, conversion to the isothiocyanate was effected by reaction with CS_2 and then desulfurization with hydrogen peroxide affords isothiocyanate **5**.^{13b} Additional methods of isothiocyanate synthesis are described for other analogs in the **Supplementary Materials**. Formation of dithiocarbamates such as **6** were achieved by reaction of the isothiocyanates with the appropriate thiol in

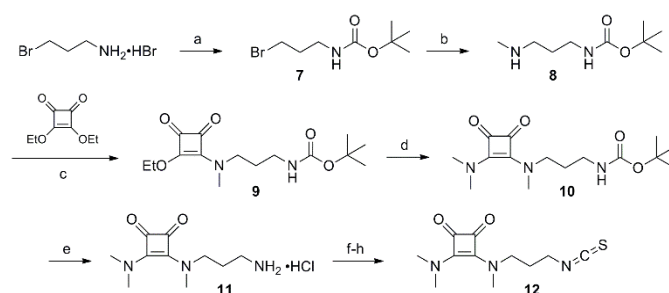


dichloromethane.

Scheme 2. General synthetic route for isonitrile and dithiocarbamates. Conditions: (a) *p*-NO₂-PhOCOCl, Et₃N, DCM, 0 to 23 °C, 57%; (b) 7-NH₂-quinoxalin-6-amine, Et₃N; (c) HCl/dioxane, 57%; (d) CS₂, Et₃N; (e) H₂O₂, 44%; (f) thiol, solvent, 44%

Multigram quantities of the lead compound **12** were prepared according to the synthetic sequence depicted in **Scheme 3**. This synthesis is six steps from the HBr salt of 3-bromopropyl amine that is commercially available, as is the subsequently formed Boc protected intermediate **7**, and the *mono*-protected diamine **8**. Preparation of the unsymmetrical squareamide takes advantage of the lowered reactivity of the *mono*-ethoxy squareamide **9** compared with diethoxysquarate. The most challenging step was the large scale isothiocyanate synthesis that was developed into an efficient and scaleable procedure using CS₂ and tosyl

chloride.^{13c} This route was used to effectively prepare multigram quantities of highly purified **12**.

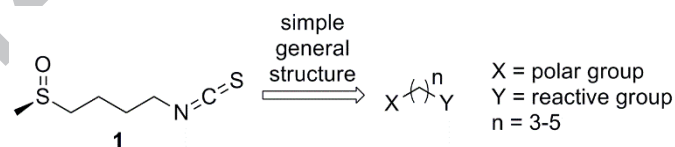


Scheme 3. Scalable synthetic route to high purity **12**. Conditions: (a) Boc₂O, Et₃N, DCM, 88%; (b) MeNH₂, THF, quant.; (c) EtOH, 97%; (d) MeNH₂·HCl, EtOH, 80 °C; (e) HCl/dioxane, 55 °C, 95%; (f) CS₂, TsCl, 50-80%; (g) SFC chromatographic purification; (h) crystallization acetone/hexanes, 85-90%

Compound design and lead identification

The starting point for SAR assessment of the sulforaphane analogs was the general structure depicted in **Chart 1** where a polar functionality is connected via an alkyl linker to a reactive group.

Chart 1. The relationship of the analogs to sulforaphane.



Efforts to replace the isothiocyanate electrophile

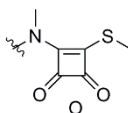
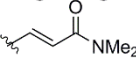
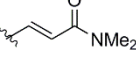
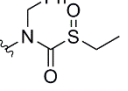
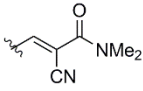
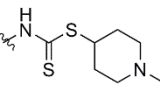
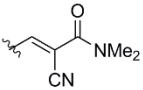
Initially, analogs of SFN, where the isothiocyanate was replaced by other potentially reactive functionality (Y in the general structure in **Chart 1**), were assessed. These analogs retain a methyl sulfoxide or a closely related methyl sulfone as depicted in **Table 1**. Our primary method for compound evaluation was a functional assay screen using normal human bronchial epithelial (NHBE) cells with a 10 μM concentration of the analog being evaluated. The level of expression of the Nrf2 pathway dependent gene heme oxygenase-1 (HO-1) was measured after a 24 h incubation with the analog and was expressed as fold-change relative to 10 μM of SFN determined in the same assay. Of note, in NHBE cells treatment with SFN resulted in approximately a 4-fold induction in HO-1 gene expression over control cells in basal state (i.e., DMSO treated) at a 10 μM concentration used in the screening assay (data not shown; see **Biological Methods** in the **Supplementary Materials** for additional assay details).

Among the reactive groups in **Table 1**, the only replacement for the isothiocyanate that was comparably effective compared to SFN was the dithiocarbamate **22**. A sulfoxylthiocarbamate analog **21** related to a set of compounds previously reported to be significantly less electrophilic compared to SFN was about 4-fold less potent in the cellular screen than SFN.¹⁶ Based on the results summarized in **Table 1**, an additional 43 dithiocarbamates (DTC) and 61 isothiocyanates (ITC) were prepared to assess the effects of varying the replacements for the polar sulfoxide (X in the general structure in **Chart 1**).¹⁷

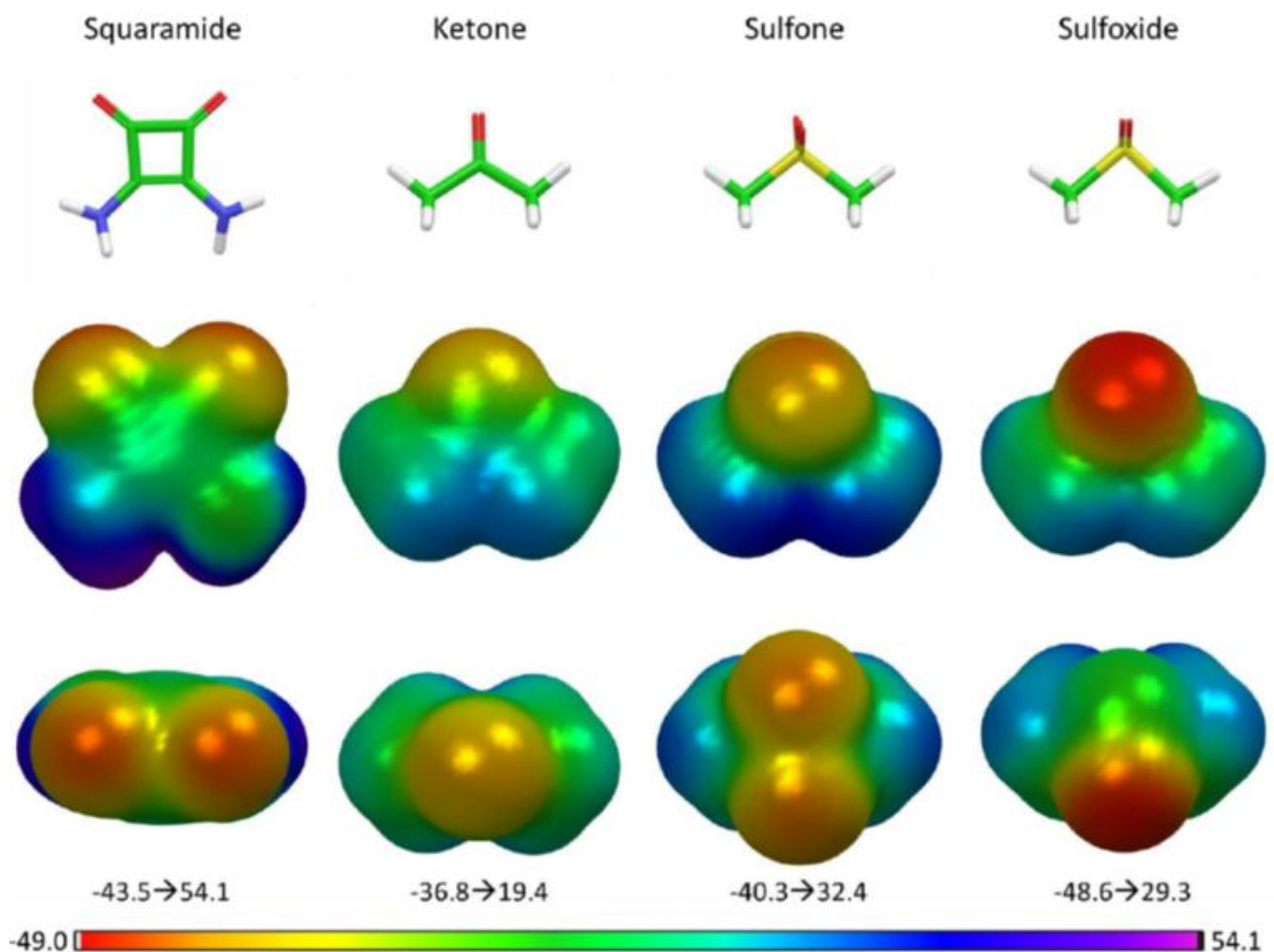
Table 1. 1 Induction of HO-1 gene expression in NHBE cells treated with diverse electrophiles, compared to (±)-SFN (**1**).^{a,b,c}



X = polar group
Y = reactive group
n = 4-5

Compound number	X	Y	n	fold-change relative to SFN	Compound number	X	Y	n	fold-change relative to SFN
(±)- 1			4	1	18			4	0.14
13			3	0.47	19			5	0.11
14			5	0.35	20			5	0.13
15			6	0.15	21			4	0.27
16			5	0.33	22			4	0.93
17			5	0.18					

^aCell assay using normal human bronchial epithelial (NHBE) cells with a 10 μ M concentration of the test article. The level of expression of the Nrf2 pathway gene, heme oxygenase-1 (HO-1), is normalized and expressed as a fold-change relative to 10 μ M of (±)-SFN (**1**). ^bSchemes and experimental procedures for the preparation of compounds **13-22** are in the **Supplementary Materials**. ^cRacemic SFN was used for analog synthesis and evaluation

Table 2. – Electrostatic potentials of polar replacements for the sulfoxide.^a

^aQuantum mechanical calculations were performed in Jaguar from Schrödinger using density functional theory (DFT) with the 6-31G** basis set to assess the electrostatic potentials of these various groups.¹⁸

Design of polar functionality for isothiocyanate and dithiocarbamate SFN analogs seeking improved properties for formulation and oral administration

The isothiocyanates and dithiocarbamates were designed with the goal of maximizing potency while retaining properties consistent with the desirable physicochemical properties required for oral administration. Some of the physicochemical features sought included crystallinity, permeability, and aqueous solubility. Given the low molecular weight of the lead compound (SFN), inclusion of amides, ureas and carbamates with aromatic substitutions was considered a viable strategy to improve crystallinity without causing unacceptably low levels of aqueous solubility. Therefore, many of the analogs synthesized and evaluated were from these classes.

Additionally, calculations of the electrostatic character of polar group replacements for the sulfoxide were undertaken to gain insight into structural features that would improve ligand binding to KEAP1. Among the analogs proposed based on this design strategy were a ketone and the novel squareamide replacement of the sulfoxide as depicted in **Table 2**.

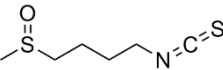
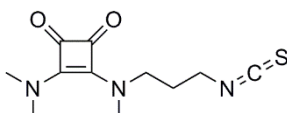
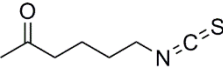
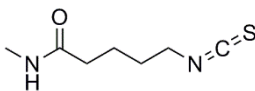
The calculations depicted in **Table 2** show the squareamide has a more negative electrostatic potential when compared to

either the ketone or sulfone and is electronically closer in character to the sulfoxide. Based on these calculations several analogs were prepared as direct SFN analogs and the potency in the NHBE cellular screen was assessed (**Table 3**). In the case of the squareamide **12**, the change in the polar feature had a noticeable impact on the cellular results. However, though the differences in this assay could be based on affinity for KEAP1, which as proposed could be related to the electronic properties of the polar group, the SAR is based on a cellular screen. Thus, the results may also be affected by other properties such as aqueous solubility and membrane permeability.

SAR and mechanistic assessment of a set of isothiocyanates and dithiocarbamates

Analysis of the data for all the isothiocyanates and dithiocarbamates with polar group variations in the NHBE cellular screen vs the Cul3/KEAP1 TR-FRET assay¹⁷ is depicted in **Figure 1**. **Figure 1** clearly shows a low correlation between the cellular potency relative to SFN (log scale) of the new isothiocyanate (ITC) and dithiocarbamate (DTC) analogs and the Cul3/KEAP1 TR-FRET assay pIC₅₀ measuring the binding of full length Cul3 and full length KEAP1.¹⁸ Furthermore, in the NHBE cellular screen using SFN as a control, HO-1 fold-change in gene expression has

Table 3. – Induction of HO-1 gene expression in NHBE cells by sulfoxide mimics designed by electrostatic comparison of the polar group.

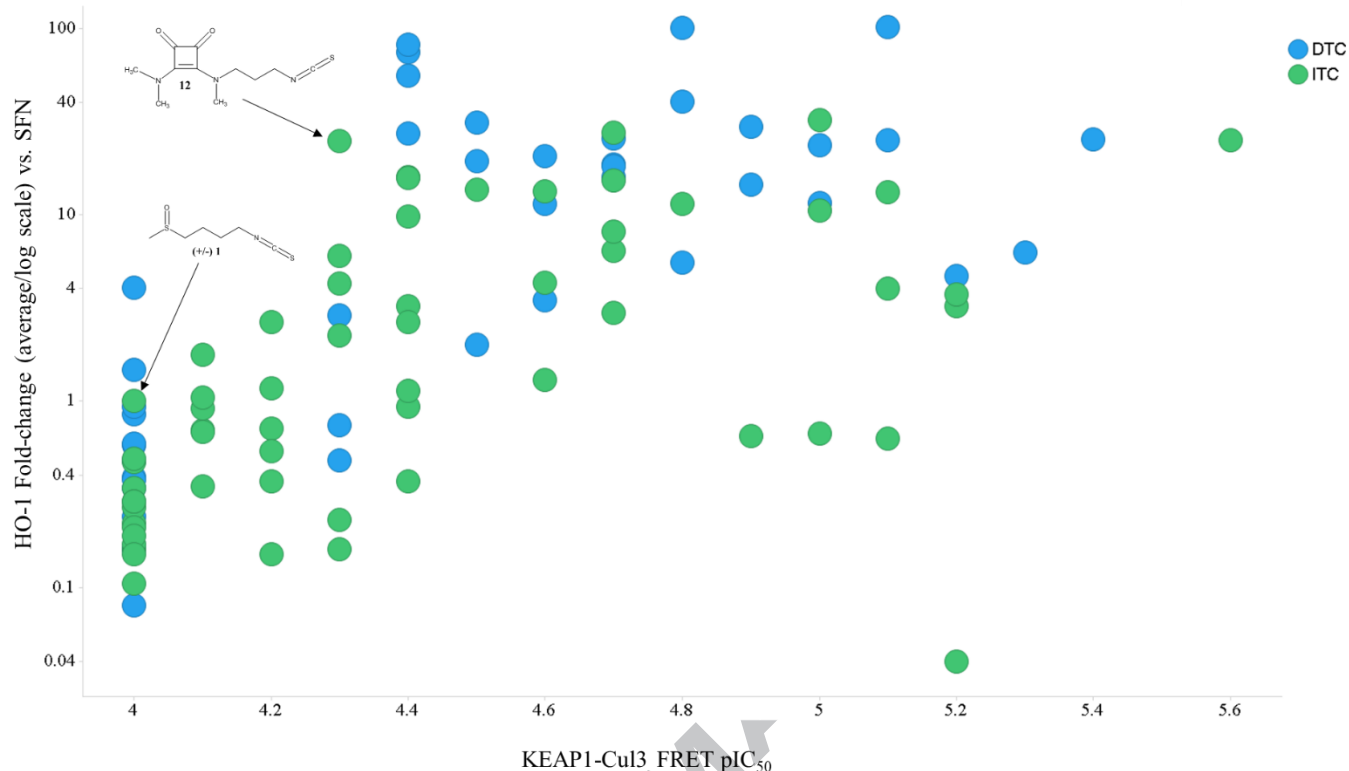
Compound number	Structure	fold-change relative to SFN ^a
(±)-1		1
12		24.9
23		0.9
24		0.7

^aCell assay using NHBE cells with a 10 μ M concentration of the test article. The level of expression of HO-1 is normalized and expressed as a fold-change relative to 10 μ M of (±)-SFN (1).

a broad window (~ 0.04-100 fold-change), while the Cul3/KEAP1 TR-FRET assay gives meaningful results over a

much narrower range (1.5 log units) and many of the analogs (including SFN) were below the limits of the Cul3/KEAP1 TR-FRET assay ($pIC_{50} < 4$). Likewise, a TR-FRET assay measuring binding of full length Nrf2 to full length KEAP1 detects no measurable activity ($pIC_{50} < 4$) for many of the analogs from this set of compounds.¹⁷ These data suggest that the biochemical assays may not be sensitive enough to measure the effects of SFN and the other analogs binding to KEAP1, but it is also possible that the analogs can inhibit the degradation of Nrf2 without disrupting the KEAP1-Cul3-Nrf2 complex¹⁹ or that the analogs are affecting HO-1 expression independent of binding to the KEAP1-Cul3-Nrf2 complex.

Figure 1. Fold-change of HO-1 gene expression in NHBE cells (average values depicted on log scale) vs. KEAP1-Cul3 TR-FRET binding data (pIC₅₀) colored by isothiocyanates (ITC) (green) and dithiocarbamates (DTC) (blue).



Given the lack of significant potency of many of the molecules in the KEAP1/Cul3 TR-FRET biochemical assay, and the fact that the SAR is based on a functional screen for increased expression of the HO-1 gene (as well as other gene products, data not shown), we sought additional support for the hypothesis that the mechanism of action of these analogs is through covalent binding to KEAP1. It has been reported that SFN binds covalently to multiple Cys residues in the BTB and IVR domains of KEAP1 including Cys151 in the BTB domain.^{2,4,19, 20,21} In order to confirm that these analogs bind KEAP1, the interaction of SFN and **12** with both wild type His-Keap1 (35-178) and mutant H6huKeap1 (35-182) C151S construct was evaluated by LC-MS. These experiments demonstrated binding of SFN and **12** to two Cys residues in the WT KEAP1 construct after a 1 h

incubation. The mass spectra show the addition products to both acetylated and non-acetylated forms of the protein construct. In contrast, incubation with the C151S mutant construct yielded only one addition product for both SFN and **12** (**Figure 2**). These data demonstrate that the isothiocyanate analogs bind to KEAP1 covalently through the BTB domain as previously reported for SFN and supports the hypothesis that disruption of the KEAP1-Nrf2-Cul3 complex is not required to increase Nrf2 cellular concentration¹⁹ and thus to increase HO-1 gene expression as shown in the cellular assay screen. Therefore, compounds potent in the cellular screen were selected for further assessment utilizing additional cellular systems.

Figure 2. Comparison of the LC-MS data for WT and mutant C151S protein with SFN and **12** after incubation for 1 h; **A.** SFN with HisKeap1 (35-178); **B.** **12** at 1 h with HisKeap1 (35-178); **C.** SFN at 1 h with H6huKeap1 (35-182) C151S; **D.** **12** at 1 h with H6huKeap1 (35-182) C151S.

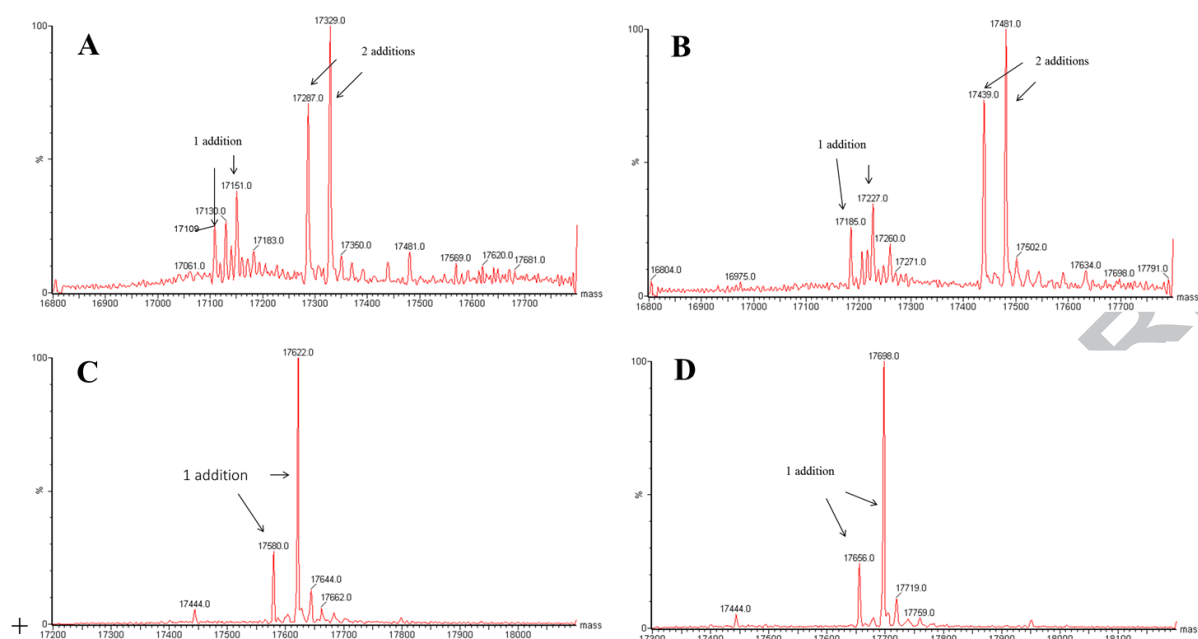


Table 4. Representative comparison of isothiocyanate its corresponding dithiocarbamate.

The structure-activity relationships (SAR) for the isothiocyanates and dithiocarbamates using the cellular screen demonstrated dependence of potency on the linker length ($n = 4$ appears optimal, see **Table 1**) as well as the polar functional group (X in **Table 1**). For the dithiocarbamates, with an additional point of structural diversity at the dithiocarbamate, the SAR is also influenced by the substitution pattern on the dithiocarbamate. In many cases, dithiocarbamates are more potent inducing the expression of the HO-1 gene than the corresponding isothiocyanates when screened at a $10 \mu\text{M}$ concentration. This trend is illustrated in **Figure 3** and an example of the relative potencies of a parent isothiocyanate and corresponding dithiocarbamate is shown in **Table 4**.

Compound number	Structure	fold-change relative to SFN ^a
(±)-1		1
5		13.2
6		101.8

^aCell assay using NHBE cells with a $10 \mu\text{M}$ concentration of the test article. The level of expression of HO-1 is normalized and expressed as a fold-change relative to $10 \mu\text{M}$ of (±)-SFN (1).

Figure 3. Induction of HO-1 gene expression by compounds screened at 10 μM (expressed relative to 10 μM SFN) for the parent isothiocyanates (ITC) (green) and corresponding dithiocarbamates (DTC) (blue) analogs.

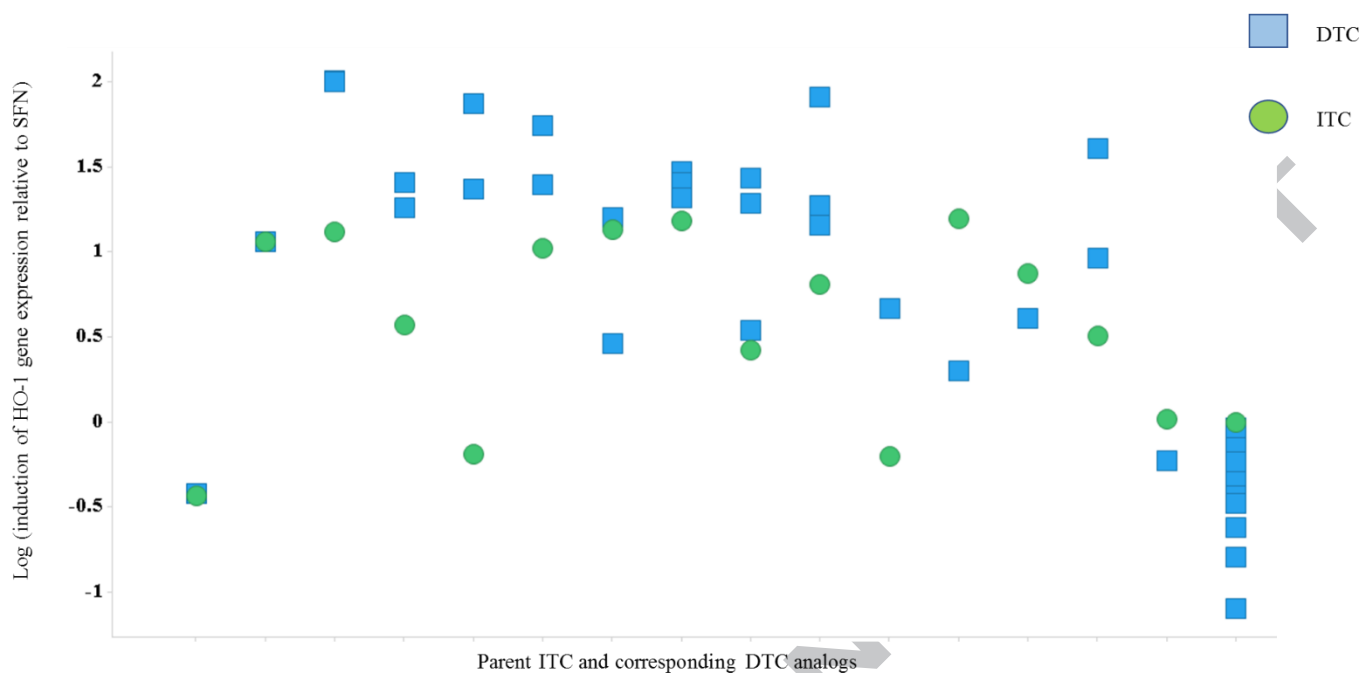
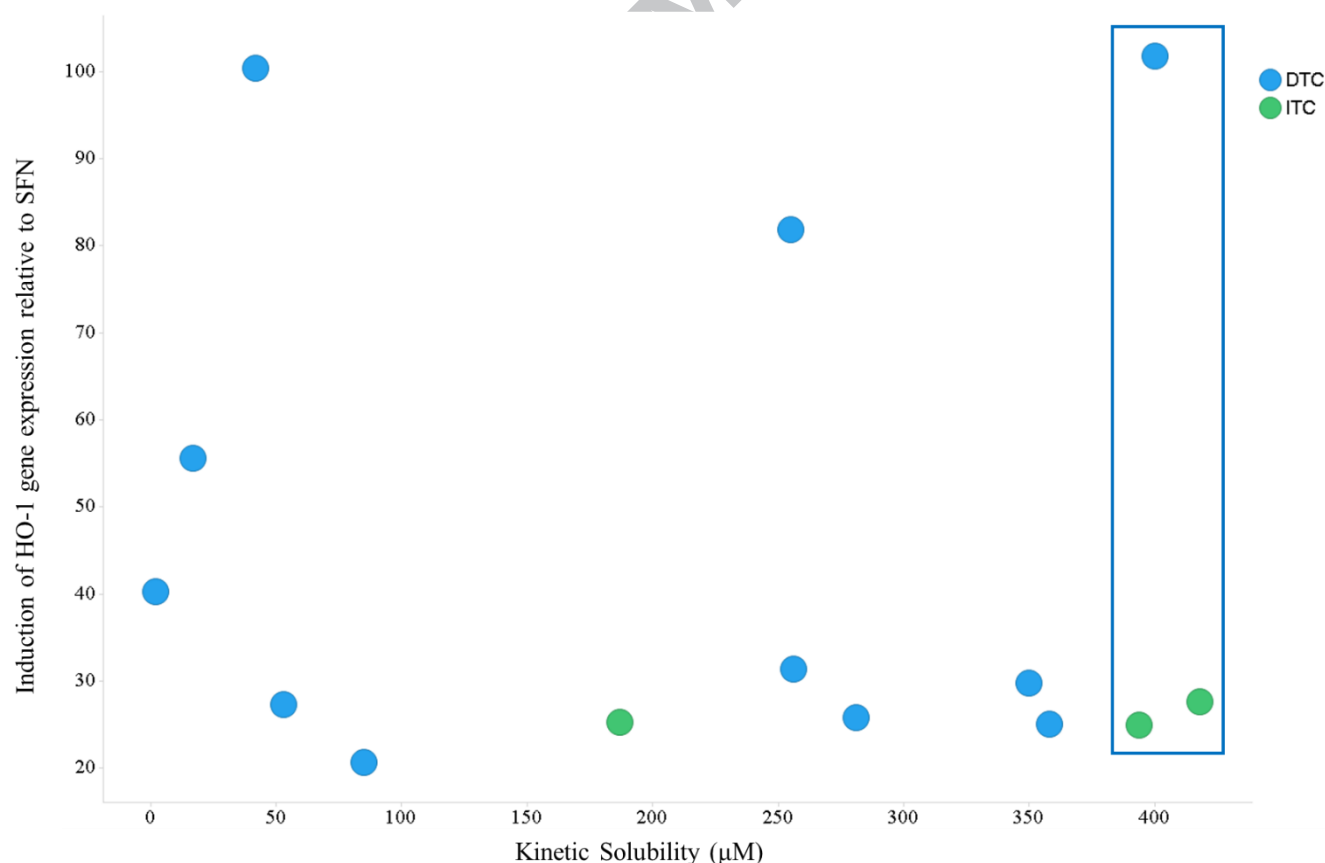


Figure 4. Induction of HO-1 gene expression by compounds screened at 10 μM (expressed relative to 10 μM SFN) vs kinetic solubility at pH 7.4 colored by isothiocyanates (ITC) (green) and dithiocarbamates (DTC) (blue).^{17, 23}



Solubility issues with the *in vivo* vehicle arose with many of the analogs selected for further evaluation based on potency in the cellular screen. The high throughput kinetic solubility (utilizing chemiluminescent nitrogen detection (CLND)) of ten of the most potent dithiocarbamates and three of the most potent

isothiocyanates from the cellular screen was evaluated (Figure 4).²³

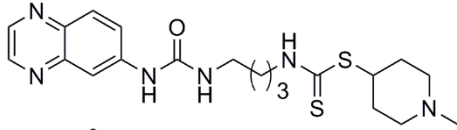
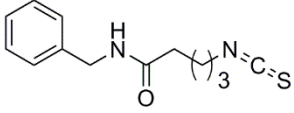
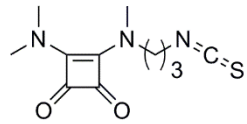
The three compounds with good kinetic solubility at pH 7.4 (compounds highlighted in the box in Figure 4) are

representative of the structures from the two chemical classes. Some of the physicochemical characteristics of these compounds are summarized in **Table 5**. Furthermore, the measured

equilibrium solubility from solid of compound **12** at pH 6.5 in fasted state simulated intestinal fluid (FaSSIF),²⁵ is relatively high, with a value of 8 mg/mL.

ACCEPTED MANUSCRIPT

Table 5. Novel analogs of SFN with good kinetic solubility and efficacy (screened at 10 μM) in the NHBE cellular screen (represented as induction of HO-1 gene expression relative to 10 μM SFN).

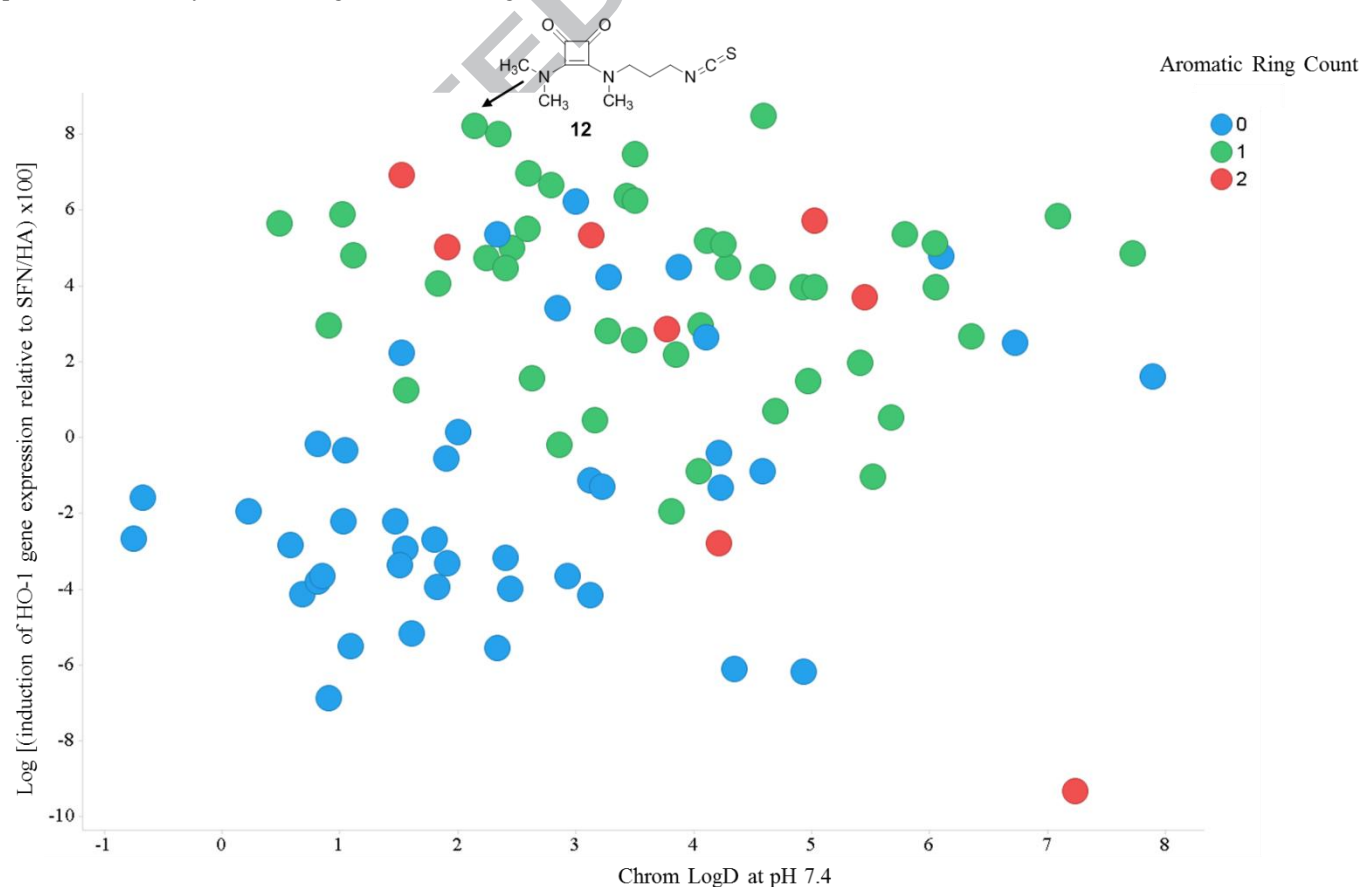
Structure	Compound number	KEAP1/CuI3 FRET pIC ₅₀	fold-change relative to SFN ^a	MW	tpsa ^b	chrom logD ²⁵	kinetic solubility ($\mu\text{g/mL}$)
	6	5.1	102	432.6	82	1.52	400
	25	4.7	28	248.3	41	4.59	418
	12	4.3	25	253.3	53	2.39	394

^aCell assay using NHBE cells with a 10 μM concentration of the test article. The level of expression of HO-1 is normalized and expressed as a fold-change relative to 10 μM of (\pm)-SFN (1). ^btpsa = topological polar surface area²⁴

To evaluate cellular potency in relation to physicochemical properties, we utilized the logarithm of the fold-change in expression level of the HO-1 gene (relative to SFN) as a relative measure of potency. Based on the concept of ligand efficiency²⁶, we utilized the log of the fold-change data from the screening assay divided by the number of heavy atoms (HA) (multiplied by 100 for better visualization) to obtain a measure of potency in the cellular screen relative to molecular size. Furthermore, when this

ratio is plotted against the chrom log D at pH 7.4 (an experimentally determined measure of lipophilicity)²⁷, the comparison affords a depiction where fold-change in cellular activity adjusted for molecular size is compared to lipophilicity, similar to lipophilic ligand efficiency (LLE) (Figure 5).^{26,28} The compounds with higher potency in the cellular screen relative to molecular size and those with lower chrom log D would be of interest as potentially developable oral Nrf2 pathway activators.

Figure 5. Log [(induction of HO-1 gene expression relative to SFN at 10 μM /number of heavy atoms(HA)) x100] vs chrom log D²⁷ at pH 7.4. Colored by aromatic ring count; blue, 0; green, 1; red, 2.



Identification of 12 as a lead compound with improved properties for formulation and oral administration

By the above criteria, **12** emerged as the most interesting compounds in the series (**Figure 5**). Compound **12** also held additional advantages such as stability as a crystalline solid (>3 years at 23 °C),²⁹ excellent FaSSIF solubility (measured from crystalline solid), moderate topological polar surface area and low molecular weight (**Table 5**). Further, the tertiary squaramide incorporated in **12** mimics similar polar tertiary urea and amide analogs. For instance, since dialkyl tertiary squaramides such as **12** can only act as H-bond acceptors and not H-bond donors³⁰ they likely mimic the difference in permeability between tertiary and secondary amides.³¹ The MDR1-MDCK permeability of **12** was considered good with $P_{app} = 12.5 \times 10^{-6}$ cm/s (A→B) and $P_{app} = 7.67 \times 10^{-6}$ cm/s (B→A).³²

Compound **12** was further evaluated relative to known Nrf2 activators in a related cellular assay that measures increase of activity of an enzymatic protein, NAD(P)H dehydrogenase [quinone] 1 (NQO1), downstream of Nrf2 activation. This assay utilizes an immortalized human bronchial epithelial (BEAS2B) cell line measuring increases in levels of NQO1 protein utilizing an NQO1 enzyme assay.³³ The results of this comparison to SFN and bardoxolone methyl (CDDO-Me)^{34,35} are depicted in **Figure 6**. Compound **12** increases the levels of NQO1 (measured by NQO1 activity) in a dose dependent manner with a potency similar to SFN. In addition, although bardoxolone methyl is considerably more potent than **12** and SFN, all three compounds display similar efficacy in the assay. Interestingly, **12** and SFN display differential upregulation of HO-1 in the NHBE cellular screen. HO-1 has a complex promoter compared to other ARE-

regulated genes, as the HO-1 gene can be regulated by several additional transcription factors including the repressor Bach1.³⁶ A potential mechanistic explanation for this observation can be attributed to the differential activity of **12** and SFN with respect to the transcriptional repressor Bach1 as determined in a cellular fragment complementation assay measuring the interaction of Bach1 and MafK. In this assay, **12** was a more potent inhibitor than SFN ($pIC_{50} = 5.5$ and 4.8, respectively) of the interaction of Bach1-MafK, an interaction required for the binding of the repressor and possibly contributing to increased HO-1 upregulation noted in the cellular screen (see Biological Methods in the Supplementary Materials for additional details).

Finally, **12** was evaluated *in vivo* utilizing a murine cigarette smoke challenge model that incorporates oxidative stress induced by cigarette smoke and which is widely used to study inflammatory responses in the airways (See Supplementary Materials section for model details). In this model, **12** dosed orally 24 h prior to the cigarette smoke challenge inhibited the influx of neutrophils in a dose dependent manner (**Figure 7**). Furthermore, the inhibitory effect of **12** on neutrophilic infiltration was comparable to the effect of SFN (**Figure 7**). Similar observations were made for both **12** and SFN with respect to inhibition of total and mononuclear cell infiltration into the airways (data not shown). Altogether, these data demonstrate that the ability of **12** to activate the Nrf2 pathway in human bronchial epithelial cells translates into dose-dependent inhibition of lung inflammation in an *in vivo* model of pulmonary oxidative stress, which might be relevant in diseases presenting with high neutrophilic-driven inflammation and oxidative stress such as COPD.³⁷

Figure 6. The comparison of analog **12**, SFN, and bardoxolone methyl in a cellular assay measuring increases of NQO1 protein utilizing a NQO1 enzymatic assay. Bardoxolone methyl (CDDO-Me): red; **12**: blue; (±) SFN: black. The corresponding pEC_{50} values are: 5.68 (SFN), 8.06 (CDDO-Me) and 5.78 (**12**).

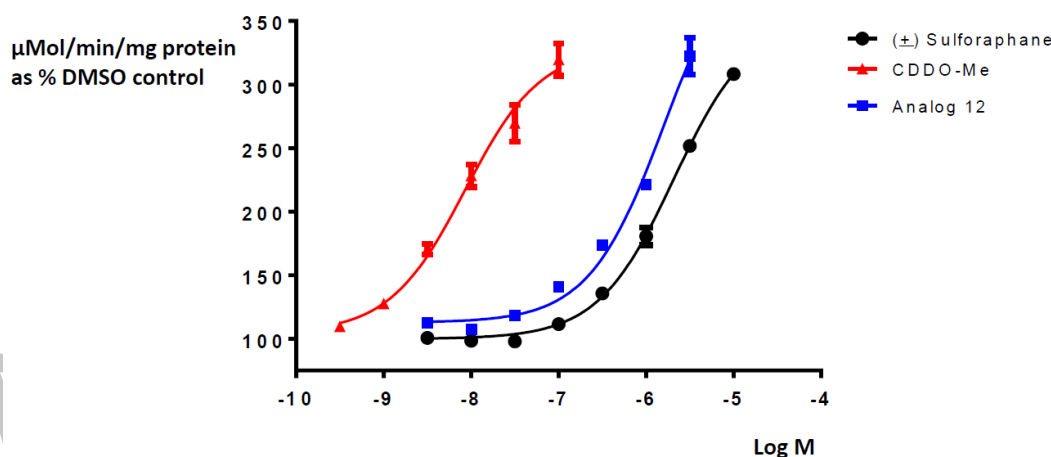
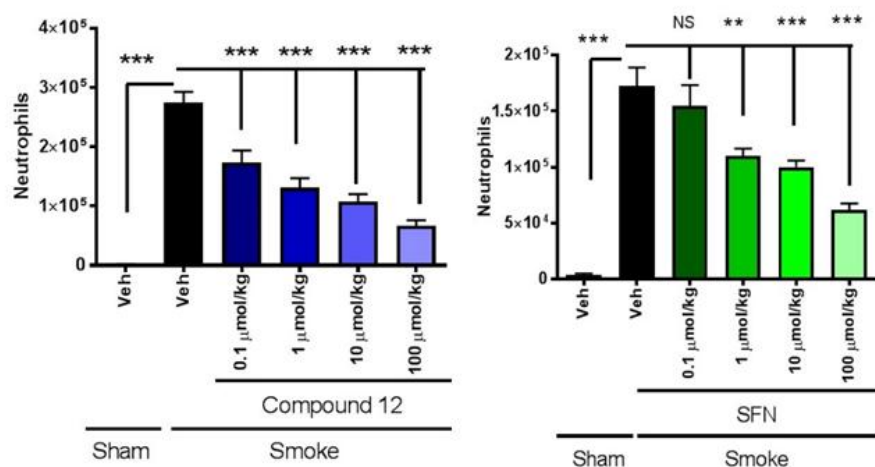


Figure 7. Inhibition of neutrophil infiltration by SFN and **12** in a cigarette smoke challenge model in mice.**Table 6.** Profile of SFN and **12** and their GSH and NAC adducts in BEAS2B cell assay determining levels of NQO1 (measured by NQO1 enzyme activity).

Compound number	Structure	pEC ₅₀	Compound number	Structure	pEC ₅₀
(+/-) 1		5.8	12		5.8
26		5.8	28		5.8
27		5.8	29		5.8

Activity was determined in BEAS2B cells by determining increase in NQO1 activity (as a measure of NQO1 protein level) after incubation of compounds for 48 h.; NAC = N-acetyl cysteine and GSH = glutathione.

When dosed orally (2 mg/kg) in a rat pharmacokinetic study, **12** displayed high systemic clearance although the major metabolites were shown to be the glutathione (GSH) **28** and N-acetylcysteine (NAC) **29** adducts of **12** (data not shown).³⁸ Taking these metabolites into consideration, oral administration does provide a high combined systemic exposure of **12** and its adducts. Using a subsequently developed high throughput version of the BEAS2B/NQO1 assay described previously, the GSH and NAC adducts of both **12** and SFN demonstrated a similar potency compared to the corresponding isothiocyanate containing parent molecules (Table 6). Thus, the activity of the adducts is consistent with the hypothesis that these isothiocyanate analogs exist in a reversible equilibrium with thiocarbonates of GSH and NAC *in vivo*.

Summary

Analogues of SFN were prepared and evaluated in a cellular screen that compared their ability to activate the Nrf2 pathway as measured by their ability to upregulate HO-1 gene expression relative to SFN. The more potent examples were then assessed for physicochemical properties desirable for their formulation and administration as oral drugs. Among the most promising analogs, the dialkyl tertiary squaramide **12** was shown to be a covalent Nrf2 activator that binds to the BTB domain of KEAP1.

Compound **12** can be isolated as a crystalline solid that displays good aqueous

solubility and long term solid phase stability. Compound **12** has demonstrated efficacy for activation of the Nrf2 pathway in BEAS2B cells that also translates to a dose-dependent inhibition of lung inflammation in an *in vivo* model of pulmonary oxidative stress. In conclusion, **12** is an orally bioavailable, efficacious, crystalline and more easily formulated analog of SFN that has been shown to activate the Nrf2 pathway both *in vitro* and *in vivo* and can function as a readily prepared tool for evaluation of the Nrf2 signaling pathway.

In addition, the use of a tertiary alkyl squaramide as a replacement for amides or ureas to increase permeability, aqueous solubility, and crystallinity, may be generally applicable to other medicinal chemistry target series.

All studies were conducted in accordance with the GSK Policy on the Care, Welfare and Treatment of Laboratory Animals and were reviewed the Institutional Animal Care and Use Committee either at GSK or by the ethical review process at the institution where the work was performed.

Acknowledgements

The authors would like to thank Nicole Goodwin for providing scientific review and helpful suggestions. GlaxoSmithKline provided funding to C.J. Moody and A.J. Wilson.

References and notes

- Boutten, A.; Goven, D.; Artaud-Macari, E.; Boczkowski, J.; Bonay, M. NRF2 targeting: a promising therapeutic strategy in chronic obstructive pulmonary disease. *Trends in Molecular Medicine* **2011** 17(7), 363–371.
- (a) Eggler, A.L.; Gay, K.A.; Mesecar, A.D.; Molecular mechanisms of natural products in chemoprevention: Induction of cytoprotective enzymes by Nrf2. *Mol. Nutr. Food Res.* **2008**, 52, S84–S94; (b) Baird, L.; Dinkova-Kostova, A. T.; The cytoprotective role of the Keap1-Nrf2 pathway *Arch Toxicol* **2011** 85, 241–272; (c) Lu, M.C.; Ji, J.A.; Jiang, Z.Y.; You Q.D.; The Keap1–Nrf2–ARE Pathway As a Potential Preventive and Therapeutic Target: An Update. *Med. Res. Rev.*, **2016**, 36, 924–963.
- An alternative to small molecule activation of the Nrf2 pathway through covalent interaction with nucleophilic cysteines on the Keap1 protein is through direct, non-covalent, competition with Nrf2 binding to the KEAP1 Kelch domain. For example see: Davies, T.G.; Wixted, W.E.; Coyle, J.E.; Griffiths-Jones C.; Hearn K.; McMenamin R.; Norton D.; Rich S.J.; Richardson C.; Saxty G.; Willems H.M.G.; Woolford A.J.-A.; Cottom J.E.; Kou J.-P.; J.G., Feldser H.G.; Sanchez Y.; Foley J.P.; Bolognese B.J.; Logan G.; Podolin P.L.; Yan H.; Callahan J.F.; Heightman T.D.; Kerns J.K.; Monoacidic Inhibitors of the Kelch-like ECH-Associated Protein 1: Nuclear Factor Erythroid 2-Related Factor 2 (KEAP1:NRF2) Protein–Protein Interaction with High Cell Potency Identified by Fragment-Based Discovery. *J. Med. Chem.* **2016** 59(8) 3991–4006.
- Zhang, D.D.; Lo, S.-C.; Cross, J.V.; Templeton, D.J.; Hannick, M. Keap1 Is a Redox-Regulated Substrate Adaptor Protein for a Cul3-Dependent Ubiquitin Ligase Complex. *Mol. And Cell. Biol.* **2004** 24(24) 10941–10953.
- In this paper where the chiral, natural isomer of sulforaphane is referred to, it will be referred to as “natural SFN”. Racemic sulforaphane was used for testing, as a synthetic intermediate for conversion to some analogs and for comparison with analogs. The racemic sulforaphane will be denoted as SFN or **1** without any further designation.
- (a) Dinkova-Kostova, A. T.; Kostov, R.V. Glucosinolates and isothiocyanates in health and disease. *Trends in Molecular Medicine* **2012** 18(6) 337–347; (b) Wittstock, U.; Halkier, B.A. Glucosinolate research in the Arabidopsis era. *Trends in Plant Science* **2002** 7(6) 263–270.
- Fahey, J.W.; Talalay, P. Antioxidant Functions of Sulforaphane: a Potent Inducer of Phase II Detoxication. *Enzymes Food and Chemical Toxicology* **1999** 37 973–979.
- Egner, P. A.; Chen, J.-G.; Zarth, A. T.; Ng, D. K.; Wang, J.-B.; Kensler, K. H.; Jacobson, L. P.; Munoz, A.; Johnson, J. L.; Groopman, J. D. Rapid and Sustainable Detoxication of Airborne Pollutants by Broccoli Sprout Beverage: Results of a Randomized Clinical Trial in China. *Cancer Prevention Research* **2014**, 7(8), 813–823.
- Doa, D.P.; Paib, S.B.; Rizvib, S.A.A.; D’Souza, M.J. Development of sulforaphane-encapsulated microspheres for cancer epigenetic therapy. *International Journal of Pharmaceutics* **2010** 386, 114–121.
- Danafar H.; Sharafi A.; Manjili H.K.; Andalib S. Sulforaphane delivery using mPEG–PCL co-polymer nanoparticles to breast cancer cells. *Pharmaceutical Development and Technology* **2017** 22(5), 642–651.
- U.S. Patent US7879822 (Stabilized Sulforaphane A method of stabilizing sulforaphane is provided. The method includes contacting sulforaphane, or an analog thereof, and a cyclodextrin to form a complex between the sulforaphane, or analog thereof, and the cyclodextrin.). U.S. Patent US20130143963 <http://evgen.com/>
- Khiar, N.; Werner, S.; Mallouk, S.; Liedler, F.; Alcudia, A.; Fernandez, I. Enantiopure Sulforaphane Analogues with Various Substituents at the Sulfinyl Sulfur: Asymmetric Synthesis and Biological Activities. *J. Org. Chem.* **2009** 74, 6002–6009.
- (a) Mukerjee, A. K.; Ashare, R. Isothiocyanates in the Chemistry of Heterocycles. *Chemistry Reviews* **1991** 91(1) 1–24. (b) Li, G.; Tajima, H.; Ohtani, T. An Improved Procedure for the Preparation of Isothiocyanates from Primary Amines by Using Hydrogen Peroxide as the Dehydrosulfurization Reagent. *J. Org. Chem.* **1997**, 62, 4539–4540. (c) Wong, R.; Dolman, S. J. Isothiocyanates from Tosyl Chloride Mediated Decomposition of in Situ Generated Dithiocarbamic Acid Salts. *J. Org. Chem.* **2007**, 72, 3969–3971. (d) Kim, S.; Yi, K.Y. 1,1'-Thiocarbonyldi-2,2'-pyridone a new useful reagent for functional-group conversions under essentially neutral conditions. *J. Org. Chem.* **1986** 2613–2615.
- Posner, G.H.; Cho, C.-G.; Green, J.V.; Zhang, Y.; Talalay, P. Design and Synthesis of Bifunctional Isothiocyanate Analogs of Sulforaphane: Correlation between Structure and Potency as Inducers of Anticarcinogenic Detoxication Enzymes. *J. Med. Chem.* **1994** 37, 170–176
- Wilson, A. J.; Kerns, J.K.; Callahan, J.F.; Moody, C.J. Keep Calm, and Carry on Covalently *J. Med Chem.* **2013**;56(19),7463–76 and references therein.
- Electrophilic tuning of the chemoprotective natural product sulforaphane. Ahn, Y.-H.; Hwang, H.; Liu, H.; Wang, X.J.; Zhankg, Y.; Stephenson, K.K.; Boronina, T.N.; Cole, R.N.; Dinkova-Kostova, A.T.; Talalay, P.; Cole, P.A. *PNAS* **2010** 107(21) 95(0–9595.
- A listing of the structures of these 104 compounds with the levels of HO-1 mRNA induced relative to SFN as well as TR-FRET data for inhibition of Cul3 binding to Keap1 are in a table attached to the Supplementary Materials. Except where noted on the Supplementary Materials experimentals, these compounds had good LC-MS data with LC purity $\geq 95\%$ and ^1H NMR data consistent with the structures.
- Poore, D. D., Hofmann, G., Wolfe III, L. A., Qi, H., Jiang, M., Fischer, M., Wu, Z., Sweitzer, T. D., Chakravorty, S., Donovan, B., Li, H. Development of a High-Throughput Cul3-Keap1 Time-Resolved Fluorescence Resonance Energy Transfer (TR-FRET) Assay for Identifying Nrf2 Activators. *SLAS Discovery*, **2018**, 1–15. <https://doi.org/10.1177/2472555218807698>.
- Baird, L., Dinkova-Kostova, A. T. Diffusion dynamics of the Keap1-Cullin3 interaction in single live cells. *Biochem. Biophys. Res. Comm.* **2013**, 433 (1), 58–65.
- Bochevarov, A.D.; Harder, E.; Hughes, T.F.; Greenwood, J.R.; Braden, D.A.; Philipp, D.M.; Rinaldo, D.; Halls, M.D.; Zhang, J.; Friesner, R.A. Jaguar A high-performance quantum chemistry software program with strengths in life and materials sciences. *Int. J. Quantum Chem.*, **2013**, 113(18), 2110–2142.
- Cleasby A., Yon J., Day P.J., Richardson C., Tickle I.J., Williams P.J., Callahan J.F., Carr R., Concha N., Kerns J.K., Qi H., Sweitzer T., Ward P., Davies T.G. Structure of the BTB Domain of Keap1 and Its Interaction with the Triterpenoid Antagonist CDDO. *PLOS ONE* <https://doi.org/10.1371/journal.pone.0098896>
- Hu, C.; Eggler, A.L.; Mesecar, A.D.; van Breemen R.B.; Modification of Keap1 Cysteine Residues by Sulforaphane. *Chem. Res. Toxicol.* **2011** 24, 515–521.
- Bhattachar, S.N.; Wesley, J.A.; Seadeek, C. Evaluation of the chemiluminescent nitrogen detector for solubility determinations to support drug discovery. *Journal of Pharmaceutical and Biomedical Analysis* **2006** 41 152–157.
- Calculated as described in Ertl P., Rohde B, Selzer P. Fast calculation of molecular polar surface area as a sum of fragment-based contributions and its application to the prediction of drug transport properties. *J Med Chem.* **2000** 43(20), 3714–3717, using software available through Chemaxon <https://chemaxon.com/>
- Augustijns, P.; Wuyts, B.; Hens, B.; Annaert, P.; Butler, J.; Brouwers, J. A review of drug solubility in human intestinal fluids: Implications for the prediction of oral absorption. *European Journal of Pharmaceutical Sciences* **2014** 57 322–332. And references therein.
- Shultz, M.D. Setting expectations in molecular optimizations: Strengths and limitations of commonly used composite parameters. *Biorg. and Med. Chem. Let.* **2013** 23, 5980–5991.
- Young, R.J.; Green, D.V.S.; Luscombe, C.N.; Hill, A.P. Getting physical in drug discovery II: the impact of chromatographic hydrophobicity measurements and aromaticity. *Drug Discovery Today* **2011** 16(17/18) 822 – 830.

28. Hopkins, A.L.; Keserü, G.M.; Leeson, P.L.; Rees, D.C., Reynolds; C.H. The Role of Ligand Efficiency Measures in Drug Discovery. *Nature Rev. Drug Disc.* **2014** 13(2): 105-121.
29. The stability was determined by checking LC-MS and ¹H NMR data after > 3 years at 23 °C in a desiccator and noting no change in the spectral data over this time.
30. Storer, R.I.; Aciro, C.; Jones, L.H. Squaramides: physical properties, synthesis and applications. *Chem. Soc. Rev.* **2011** 40, 2330–2346.
31. Conradi, R.A.; Hilgers, A.R.; Ho, N.F.H.; Burton, P.S. The Influence of Peptide Structure on Transport Across Caco-2 Cells. II. Peptide Bond Modification Which Results in Improved Permeability. *Pharm. Res* **1992** 9, 435 – 439.
32. (a) Volpe, D.A. Drug-permeability and transporter assays in Caco-2 and MDCK cell lines. *Future Med. Chem.* **2011** 3(16), 2063–2077; (b) Thiel-Demby, V.E.; Humphreys, J.E.; St. John Williams, L.A.; Ellens, H.M.; Shah, N.; Ayrton, A.D.; Polli, J.W. Biopharmaceutics Classification System: Validation and Learnings of an in Vitro Permeability Assay. *Molecular Pharmaceutics* **2008** 6, 11–18.
33. Dinkova-Kostova, A. T.; Liby, K.T.; Stephenson, K.K.; Holtzclaw, W.D.; Xiangqun Gao, X.; Suh, N.; Charlotte Williams, C.; Risingsong, R.; Tadashi Honda, T.; Gordon W. Gribble, G.W.; Sporn, M.B.; Talalay, T. Extremely potent triterpenoid inducers of the phase 2 response: Correlations of protection against oxidant and inflammatory stress. *Proc. Natl. Acad. Sci. U.S.A.* **2005** 102 (12) 4584–4589.
34. Liby, K. T.; Sporn, M. B. Synthetic oleanane triterpenoids: multifunctional drugs with a broad range of applications for prevention and treatment of chronic disease. *Pharmacol. Rev.* **2012**, 64, 972–1003.
35. Sporn, M. B.; Liby, K. T.; Yore, M. M.; Fu, L.; Lopchuk, J. M.; Gribble, G. W. New synthetic triterpenoids: potent agents for prevention and treatment of tissue injury caused by inflammatory and oxidative stress. *J. Nat. Prod.* **2011**, 74, 537–545.
36. Zhou Y, Wu H, Zhao M, Chang C, Lu Q. The Bach Family of Transcription Factors: A Comprehensive Review. *Clin Rev Allergy Immunol.* **2016**, 50(3), 345-56.
37. Barnes, P.J. Inflammatory mechanisms in patients with chronic obstructive pulmonary disease. *J Allergy Clin Immunol.* **2016**, 138(1), 16-27.
38. Perez, H.L.; Junnotula, V.; Knecht, D.; Nie, H.; Sanchez, Y.; Boehm, J.C.; Booth-Genthe, C.; Yan, H.; Davis, R.; Callahan, J.F. Analytical approaches for quantification of a Nrf2 pathway activator: overcoming bioanalytical challenges to support a toxicity study. *Analyst* **2014**, 139, 1902-1912.

Supplementary Data

Supplementary data associated with this article can be found, in the online version, at <https://doi.org/10.1016/j.bmc.2018.01.005>.

Experimental procedures for all the chemical structures appearing in the Schemes and tables and biological methods and a table containing the listing of the structures of the isothiocyanates and dithiocarbamates included in Figures 1, 3, 4 and 5 with the levels of induced HO-1 gene expression (screened at 10 μM) relative to 10 μM SFN as well as TR-FRET data for inhibition of Cul3 and NRF2 binding to KEAP1 are included as Supplemental Materials. All compound structures are supported by LC-MS data with LC purity ≥ 95% and ¹H NMR data.

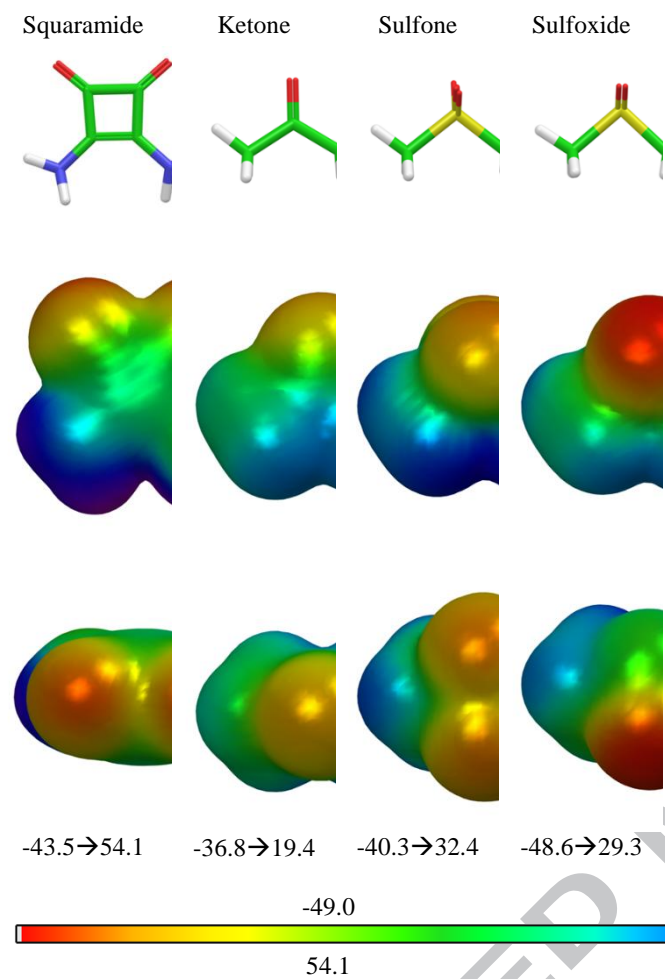
Abbreviations Used

SFN, sulforaphane; KEAP1, Kelch-like ECH-associated protein 1; GSH, glutathione; NAC, N-acetyl cysteine; NHBE, Normal Human Bronchial Epithelial cells; NQO1, NAD(P)-H:quinone acceptor oxidoreductase 1; Nrf2, Nuclear factor erythroid 2-related factor 2; BEAS2B; Bronchial epithelium + Adenovirus 12-SV40 virus hybrid (Ad12SV40), an immortalized human bronchial epithelial cell line; COPD, chronic obstructive pulmonary disease.

Table 1. Induction of HO-1 gene expression in NHBE cells treated with diverse electrophiles, compared to (\pm)-SFN (**1**).^{a,b,c}

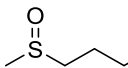
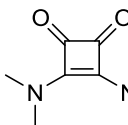
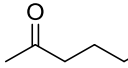
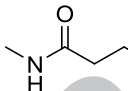
Compound Number	X	Y	n	fold-change relative to SFN	Compound Number	X	Y	n	fold-change relative to SFN
(\pm)- 1			4	1	18			4	0.14
13			3	0.47	19			5	0.11
14			5	0.35	20			5	0.13
15			6	0.15	21			4	0.27
16			5	0.33	22			4	0.93
17			5	0.18					

^aCell assay using normal human bronchial epithelial (NHBE) cells with a 10 μ M concentration of the test article. The level of expression of the Nrf2 pathway gene, heme oxygenase-1 (HO-1), is normalized and expressed as a fold-change relative to 10 μ M of (\pm)-SFN (**1**). ^bSchemes and experimental procedures for the preparation of compounds 13-22 are in the Supplementary Materials. ^cRacemic SFN was used for analog synthesis and evaluation

Table 2. Electrostatic potentials of polar replacements for the sulfoxide.^a

^aQuantum mechanical calculations were performed in Jaguar from Schrödinger using density functional theory (DFT) with the 6-31G** basis set to assess the electrostatic potentials of these various groups.¹⁸

Table 3. – Induction of HO-1 gene expression in NHBE cells by sulfoxide mimics designed by electrostatic comparison of the polar group.

Compound Number	Structure	fold-change relative to SFN ^a
(±)-1		1
12		24.9
23		0.9
24		0.7

^a Cell assay using NHBE cells with

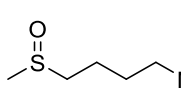
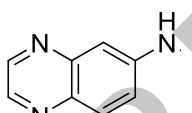
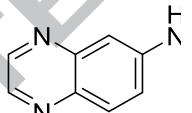
a 10 μ M concentration of the test article. The level of expression was

f
H
O
-
l
i
s
n
o
r
m
a
l
i
z
e
d
a
n
d
e
x
p
r
e
s
s
e
d
a
s
a
f
o
l
d
-
c
h
a
n
g
e
r
e
l
a
t
i
v
e
t
o
1
0

μ
M
o
f
(
 \pm
)
-
S
F
N
(
1
)
.

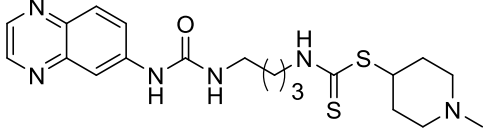
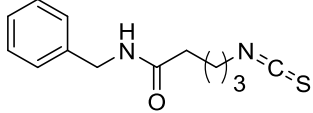
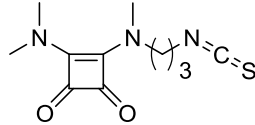
ACCEPTED MANUSCRIPT

Table 4. Representative comparison of isothiocyanate its corresponding dithiocarbamate

Compound Number	Structure	fold-change relative to SFN ^a
(±)-1		1
5		1.32
6		1.08

^aCell assay using NHBE cells with a 10 μ M concentration of the test article. The level of expression of HO-1 is normalized and expressed as a fold-change relative to 10 μ M of (±)-SFN (1).

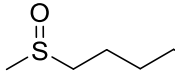
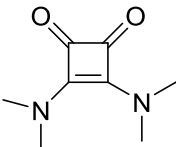
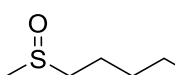
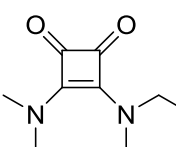
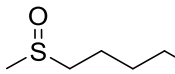
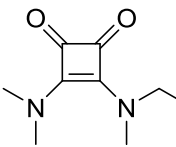
Table 5. Novel analogs of SFN with good kinetic solubility and efficacy (screened at 10 μM) in the NHBE cellular screen (represented as induction of HO-1 gene expression relative to 10 μM SFN).

Structure	Compound Number	KEAP1/Cul3 FRET pIC_{50}	fold-change relative to SFN ^a	MW	tpsa ^b	Chrom logD ²⁵	kinetic solubility (μM)
	6	5.1	102	432.6	82	1.52	≥ 400
	25	4.7	28	248.3	41	4.59	≥ 418
	12	4.3	25	253.3	53	2.39	≥ 394

^aCell assay using NHBE cells with a 10 μM concentration of the test article. The level of expression of HO-1 is normalized and expressed as a fold-change relative to 10 μM of (\pm)-SFN (1).

^btpsa = topological polar surface area.²²

Table 6. Profile of SFN and 12 and their GSH and NAC adducts in BEAS2B cell assay determining levels of NQO1 (measured by NQO1 enzyme activity).

Compound Number	Structure	PE C ₅ 0	Compound Number	Structure	PE C ₅ 0
(±)-1		5.8	12		5.8
26		5.8	28		5.8
27		5.8	29		5.8

Activity was determined in BEAS2B cells by determining increase in NQO1 activity (as a measure of NQO1 protein level) after incubation of compounds for 48 h.; NAC = N-acetyl cysteine and GSH = glutathione.